

# Friction and wear behaviour of Kevlar fabrics

M. A. MARTÍNEZ, C. NAVARRO, R. CORTÉS, J. RODRÍGUEZ,  
V. SÁNCHEZ-GÁLVEZ

*Department of Materials Science, E.T.S. Ingenieros de Caminos, Canales y Puertos,  
Polytechnic University of Madrid, Ciudad Universitaria s/n, 28040 Madrid, Spain*

Experimental results of a number of tribological tests carried out on aramid woven fabrics are presented in this paper. Kevlar Ht, Kevlar 29 and Kevlar 49 aramid plain fabrics were employed in this work. The friction and wear phenomena of the fabrics were investigated, considering both fabric–fabric and metal–fabric interaction. From the experimental data, the evolution of parameters such as static and dynamic friction coefficients, dissipated energy, volume loss of the material, wear rate, specific wear and wear strength were studied. Moreover, values of the static force needed to pull out a single fibre from the woven fabric were measured. All these data are important for the numerical modelling of impact on such materials. In fact, experimental findings on yarn failure mechanisms show that apart from tensile rupture, failure modes such as cutting, shearing and fibre degradation take place in fabrics subjected to the ballistic impact of low- and medium-calibre ammunition.

## 1. Introduction

A large amount of effort has been devoted to studying the problem of ballistic impact on woven cloth. Empirical attempts to relate the ballistic fabric efficiency to the thickness or weight of the fabric target have been made from the early stages of research on impact on fabric [1]. One of the most popular fabrics used in experimental studies on ballistic applications, together with nylon cloth, is aramid fibre. Panels composed of multiple plies of aramid cloth have been found to give sufficient protection against ballistic impact with an important saving of weight. Measurements of the ballistic limits on aramid cloth armours [2] and nylon ballistic panels [3] have been reported. Recently, numerical and analytical tools have been developed for accurate modelling of impact problems in continuous and homogeneous materials, such as metals and ceramics. However, for projectile impact on fabrics or composites, a rigorous modelling of the perforation process is not simple, and this has not yet been achieved given the difficulties in dealing with material discontinuities inherent in such materials. So the application of continuum mechanics to this type of problem is not straightforward. Approximate analytical models for projectile impact on fabrics have been developed by Leech and Adeyefa [4] and Roylance [5], who pointed out the main difficulties of the problem: (a) discontinuous contact, friction and attrition processes between neighbouring fabric plies; (b) friction and wear processes at the fabric–projectile interface, and (c) the effect of fabric crossovers on stress wave propagation in fibres, including slippage phenomena between warp and filling yarns.

The contact effects between two consecutive fabric plies may be observed clearly in the fabric zones near the projectile edge where the maximum pressure between neighbouring plies occurs. The friction and

wear processes between the fabric ply and the projectile in the impact zone can also be verified in a post-impact inspection. From direct observation of 9 mm Parabellum and 0.357 Magnum projectiles impacted on a set of Kevlar fabric layers, it is seen that plastic projectile deformation caused by friction at the projectile–fabric interface takes place. Also, failure of fibres due to yarn degradation caused by friction processes and the high temperatures generated has been experimentally observed. In this way, so-called “chunks” of degraded yarns are seen to remain in close contact with the deformed projectile after impact.

Fabric crossovers also affect the propagation of both the longitudinal tension and the transversal waves, and thus the dynamic behaviour of fabrics. This is due to local impedance and unit mass changes at the crossovers. Furthermore, the slippage between a warp and a filling yarn can change the diverted and transmitted wave energies and should also be taken into account. So a study of the tribological behaviour of aramid fabrics such as Kevlar Ht, Kevlar 49 and Kevlar 29 is of great interest in facing impact problems. However, this aspect has not been sufficiently studied in the past. Some researchers have studied the wear behaviour of fibres employed in ordinary textile applications [6–8], whereas others have concentrated on the friction and wear behaviour of fibre-reinforced composites employed in engineering applications [9–12]. An important topic such as the friction effect between isolated aramid yarns was only recently studied by Briscoe and Motamedi [13], who studied the inter-yarn friction effect at a crossover of mutually perpendicular cotton and aramid fibres by means of the point contact and the hanging fibre method. However, to the authors' knowledge, no information regarding friction and wear of aramid fabrics is currently available in the literature.

The aim of this paper is to present a set of experimental results obtained from friction and dynamic wear tests of Kevlar Ht, Kevlar 49 and Kevlar 29 fabrics. Firstly, static mutual friction coefficients are estimated for each fabric. Moreover, the force required to completely pull out a yarn from the aramid fabric is measured, giving an approximate idea of the resistance to slip of each of the aramid fabrics considered. The dynamic wear tests involve fabric-to-fabric contact and fabric-to-metal interaction. In this latter case, steel, aluminium, brass and lead are considered.

## 2. Experimental procedure and results

On reception, the Kevlar Ht, Kevlar 49 and Kevlar 29 fabrics were protected against light and moisture by putting them into black bags. The laboratory environmental conditions for all tests performed in this work were 303 K and relative humidity 50%. Some preliminary conventional quasi-static tension tests were carried out to characterize the material using a universal testing machine Suzpecar MEM-101. The elongation rate was 2 mm min<sup>-1</sup>. The single-ply fabric specimens were 400 mm long and 50 mm wide. In order to prevent fabric failure at grips, the loading boundaries of the fabric were impregnated with epoxy resin so that the jaws of the grips did not damage the specimens and these failed in the middle. Data from the above experiments, as well as others obtained from the manufacturer (E.I. Du Pont de Nemours International S.A.), are presented in Table I.

Initially, the static friction coefficients between two plies of the same kind of fabric were determined for the three types of aramid fabric considered, following the recommendations and suggestions of ASTM standard D4917 (15.09). So, a square ply of 10 cm edge was fixed to a horizontal table and a second ply was put in dry contact over it, with a weight over them to keep the interface under normal load. In the experiments, weights having masses of 0.638, 1.0916 and 1.5452 kg were used alternatively to apply the contact force. Then by means of a thread passing through a pulley and connecting the fabric to a vertically hanging weight, increasing horizontal loads were applied to the second ply by simply increasing the weight at the

opposite end of the thread, until gliding between plies finally occurred. The ratio between the friction force and the contact force was found to be nearly independent of the value of the latter, and the experimentally obtained values for such ratios (that is, for the friction coefficient  $\mu_{\text{static}}$ ) are indicated in the first row of Table II. We see in this table that Kevlar 29 has the highest mutual friction coefficient, followed by Kevlar Ht and Kevlar 49, in that order. This is due to the fact that the Kevlar 29 fabrics used in this work are more closely woven than the other fabrics. So, they present a rougher surface and it is natural to expect a higher value of the mutual friction coefficient in such conditions.

In addition, simple pull-out tests were performed to measure the static force required to completely pull out a single yarn of the fabric. The experimental set-up was similar to that described above, except that a single ply was used. The two boundaries parallel to the yarn to be pulled out were fixed to the table, and weights were located on the ply to avoid distortion during the test. One end of the thread was tied to a yarn of the fabric, and the weight was increased until pull-out of the yarn finally took place. An aspect of a Kevlar Ht fabric after the experiment is shown in Fig. 1. So, the friction force per yarn crossover and the friction force per unit length of the yarn were computed. These values are indicated in the second and third rows of Table II. We can appreciate that the force per crossover to pull out a single yarn in Kevlar 29 fabrics is about twice that needed for Kevlar 49 and Kevlar Ht, whereas the pull-out force per unit length of fibre is three to four times greater for Kevlar 29 than for Kevlar Ht or Kevlar 49. As before, this is because the Kevlar 29 fabrics tested are more closely woven

TABLE I Properties of materials

Yarns <sup>a</sup>	Kevlar Ht	Kevlar 29	Kevlar 49
Area (mm <sup>2</sup> )	0.0766	0.0766	0.111
Linear density (dtex)	1100	1100	1270
Tenacity (GPa)	3.4	2.95	2.95
Elongation at break (%)	3.3	3.3	2.4
Young's modulus (GPa)	100	79	110
<b>Fabrics<sup>b</sup></b>			
Surface density (g m <sup>-2</sup> )	190	280	220
Number of yarns per cm	8.5	12.2	6.7
Tenacity (N m <sup>-1</sup> )	1430	1680	1750
Elongation at break (%)	3.2	3.0	3.0
Young's modulus (GPa)	78	51	84

<sup>a</sup>Data from the manufacturer.

<sup>b</sup>All taffeta.

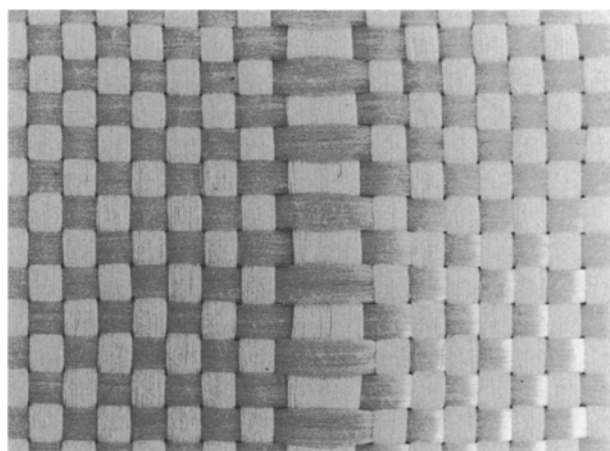


Figure 1 A view of Kevlar Ht fabric after a pull-out test.

TABLE II Frictional data

	Kevlar HT	Kevlar 29	Kevlar 49
$\mu_{\text{static}}$	0.47	0.51	0.41
Force per yarn crossover (N)	0.043	0.103	0.044
Force per cm of fabric (N)	0.365	1.257	0.295

than the others, probably resulting in greater inter-yarn pressures after manufacture.

Dynamic wear tests were carried out using a model TE-77 high-frequency Cameron-Plint friction test machine. To prevent any stretching of the fabrics during the experiments, both fabric specimens were fixed to metallic plates by means of epoxy resin. In this way the fabric was placed on the metallic plate without any initial stress. A scheme of the experimental device is seen in Fig. 2. The normal contact force between the two plies was alternatively of 10, 15 or 25 N, corresponding to normal pressures of 2.0, 3.0 and 5.0 kPa, respectively. The relative motion between the two plies had an amplitude of 15 mm and a frequency of 2.5 Hz. The contact area was about 49.5 cm<sup>2</sup>. The duration of each test, performed for dry contact only, was between 2 and 8 h. The contact interface was periodically cleaned of fabric debris during the experiments. Results obtained for Kevlar Ht are presented in Figs 3 to 6. In Fig. 3 the dynamic friction coefficient  $\mu_d$ , computed as the ratio between the recorded shear force and the normal force, is plotted as a function of the total wear path for selected values of the normal pressure at the interface. For a contact pressure of 2.0 kPa, the tendency of this parameter is to remain relatively constant, whereas for a normal pressure of 3.0 kPa a monotonic increase in the dynamic friction coefficient with the path length is observed. For a normal pressure of 5.0 kPa, after an initial stage where the value of  $\mu_d$  varies little, a sudden increase in the value of this parameter is observed. In Fig. 4, the energy dissipated by friction is

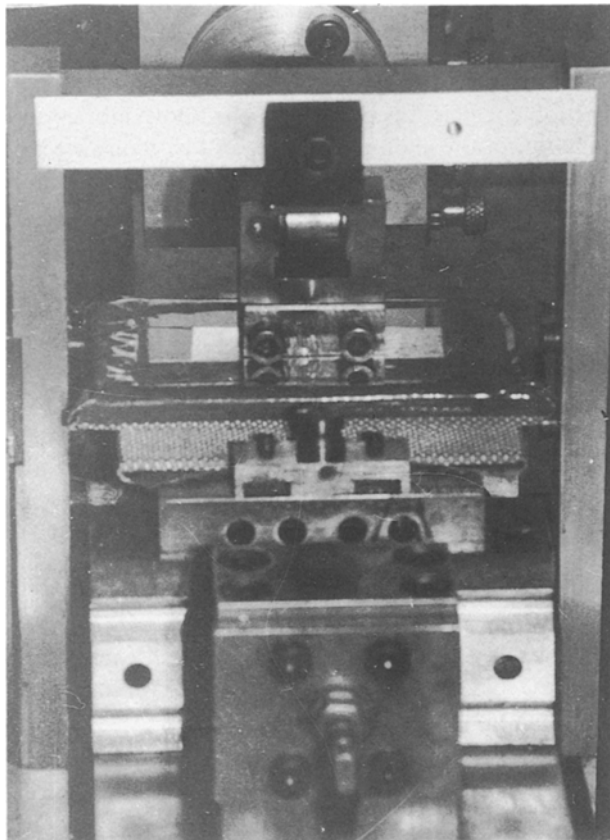


Figure 2 Experimental set-up for dynamic wear tests for fabric-fabric contact.

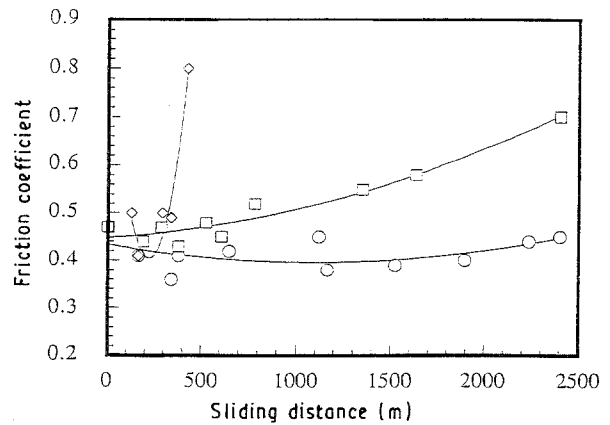


Figure 3 Mutual friction coefficient for Kevlar Ht as a function of sliding distance, for a normal pressure of (○) 2 kPa, (□) 3 kPa and (◇) 5 kPa.

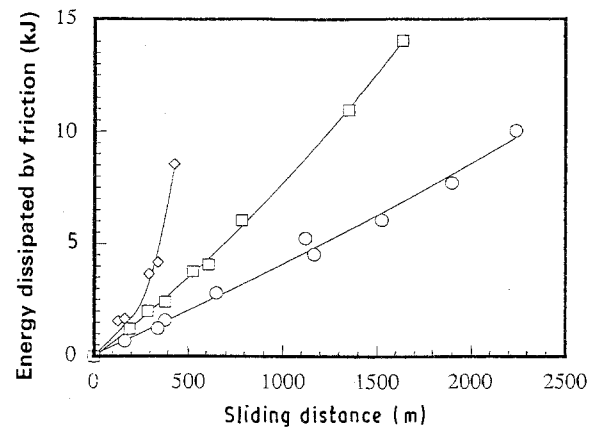


Figure 4 Energy dissipated by friction for Kevlar Ht as a function of sliding distance, for a normal pressure of (○) 2 kPa, (□) 3 kPa and (◇) 5 kPa.

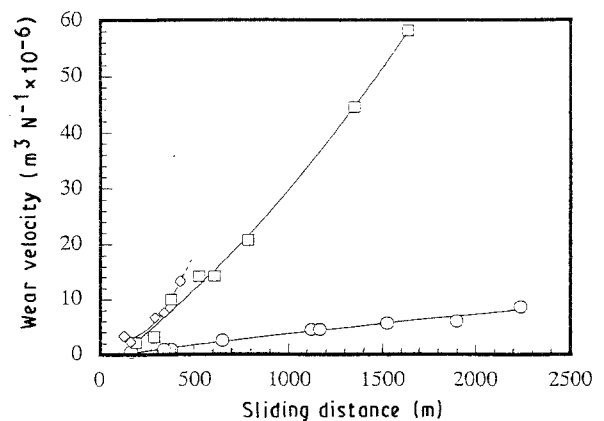


Figure 5 Wear velocity for Kevlar Ht as a function of sliding distance, for a normal pressure of (○) 2 kPa, (□) 3 kPa and (◇) 5 kPa.

plotted as a function of the total sliding distance. We see in this figure that a linear relationship fits the experimental data well for normal pressures of 2.0 and 3.0 kPa, whereas for a normal pressure of 5.0 kPa the corresponding curve has a marked upward concavity.

The wear velocity, defined as the material volume loss per unit of normal load, is depicted in Fig. 5 as a function of the sliding distance, for the different values

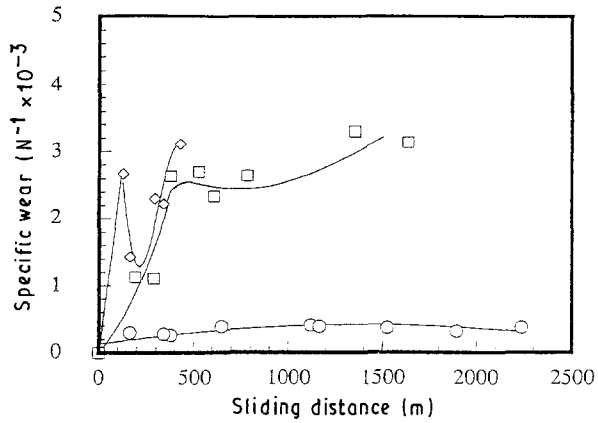


Figure 6 Specific wear for Kevlar Ht as a function of sliding distance, for a normal pressure of (○) 2 kPa, (□) 3 kPa and (◇) 5 kPa.

of the normal pressure considered in this study. We see in this figure that linear relationships fit relatively well with the experimental data. Finally, in Fig. 6 the specific wear (volume loss per unit area, unit relative sliding and unit normal load) is plotted as a function of the sliding distance. In this latter figure we can appreciate important quantitative differences between the case of a normal pressure of 2.0 kPa, and those corresponding to normal pressures of 3.0 and 5.0 kPa.

In Figs 7 to 10, results for Kevlar Ht, Kevlar 49 and Kevlar 29 for a normal pressure value of 1.2 kPa are

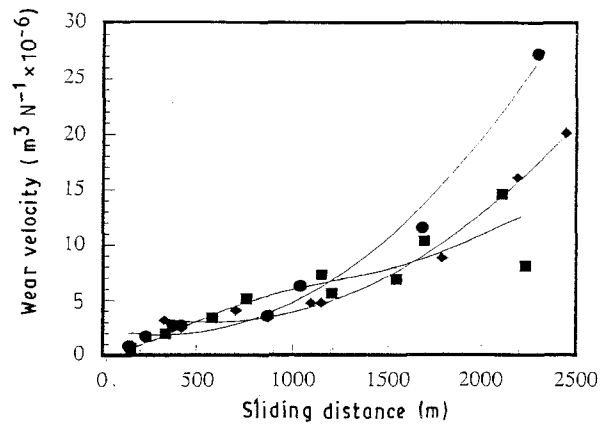


Figure 9 Wear velocity for (●) Kevlar Ht, (■) Kevlar 29 (◆) and Kevlar 49 as a function of sliding distance, for a normal pressure value of 1.2 kPa.

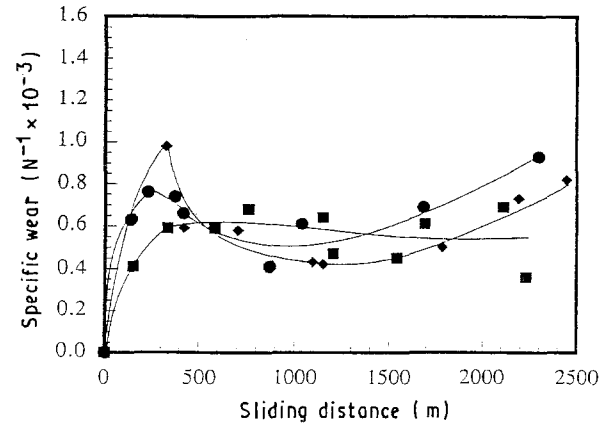


Figure 10 Specific wear for (●) Kevlar Ht, (■) Kevlar 29 and (◆) Kevlar 49 as a function of sliding distance, for a normal pressure value of 1.2 kPa.

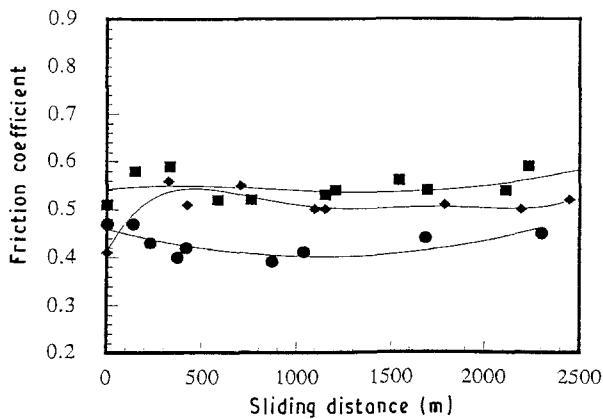


Figure 7 Mutual friction coefficient for (●) Kevlar Ht, (■) Kevlar 29 and (◆) Kevlar 49 as a function of sliding distance, for a normal pressure value of 1.2 kPa.

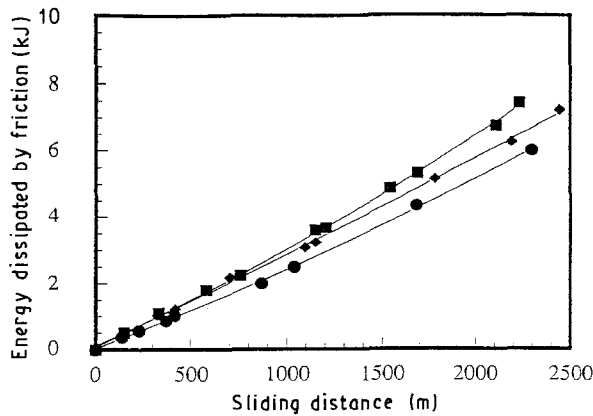


Figure 8 Energy dissipated by friction for (●) Kevlar Ht, (■) Kevlar 29 and (◆) Kevlar 49 as a function of sliding distance, for a normal pressure value of 1.2 kPa.

graphically compared. In Fig. 7 the dynamic mutual friction coefficient is plotted for the above fabrics as a function of the sliding distance. In this figure we can appreciate that whereas a decrease in the friction coefficient takes place initially in the case of Kevlar Ht, an initial increase of the friction coefficient is observed for the cases of Kevlar 49 and Kevlar 29. This means that the static friction coefficient is initially higher than the dynamic one for Kevlar Ht, whereas it is lower for Kevlar 49 and Kevlar 29. In Fig. 8, the energy dissipated by friction is shown as a function of the total sliding path, and we can see that a linear relationship reasonably approximates to the experimental measurements. In Fig. 9, the wear velocity is depicted as a function of the sliding distance for the above fabrics, showing relatively similar values for them all within the range studied. Finally, in Fig. 10 the specific wear is plotted as a function of the sliding distance for the above materials, where it can be seen that the parameter has similar values for the three aforementioned types of fabric.

Dynamic wear tests for a dry aramid-metal interface were also made. Steel, aluminium, brass and lead were employed in these experiments. This selection covers very well the type of materials used for low- and medium-calibre ammunition. The tests were carried out in the aforementioned Cameron-Plint friction test

machine. The fabric sample was fixed to a metallic plate as before. The experimental device is shown in Fig. 11. The cylindrical metal sample had a cross-sectional area of  $1.13 \text{ cm}^2$  and was attached to the moving part of the testing machine. Metal–fabric cutting effects were avoided by polishing the edges at the perimeter of the base of the specimen in contact with the fabric ply. Wear tests at different contact pressures were carried out for all the metals used in this work. Moreover, tests with different values of the relative velocity between metal and fabric were also made for steel only. For the first type of test the normal contact force was between 4.5 and 250 N, i.e., the contact pressure ranged from 0.04 to 2.2 MPa. The frequency used was 3 Hz and the amplitude of the relative displacement at the contact interface was 15 mm. The duration of this type of test was about 180 s. The sequence of tests at different relative sliding velocities was completely analogous to the previous one. In such sequence the normal metal–fabric contact pressure was kept constant and equal to 0.44 MPa, and the sliding velocity between metal and the aramid fabric ranged from 0.05 to  $1.6 \text{ m s}^{-1}$ . The evolution of the dynamic friction coefficient with normal pressure for the aramid–metal interface for the different metals considered is shown in Fig. 12 for Kevlar Ht, in Fig. 13 for Kevlar 29, and in Fig. 14 for Kevlar 49. In such

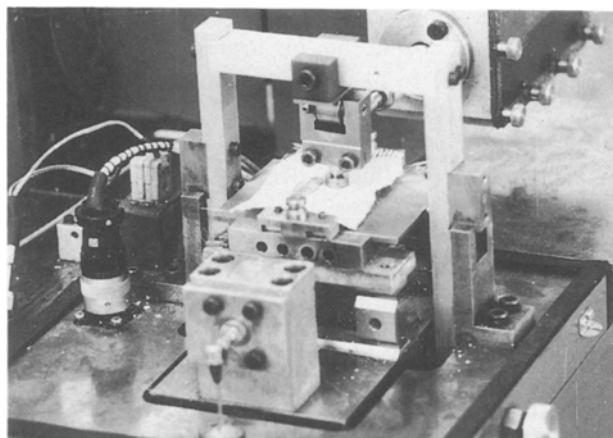


Figure 11 Experimental set-up for dynamic wear tests for fabric–metal contact.

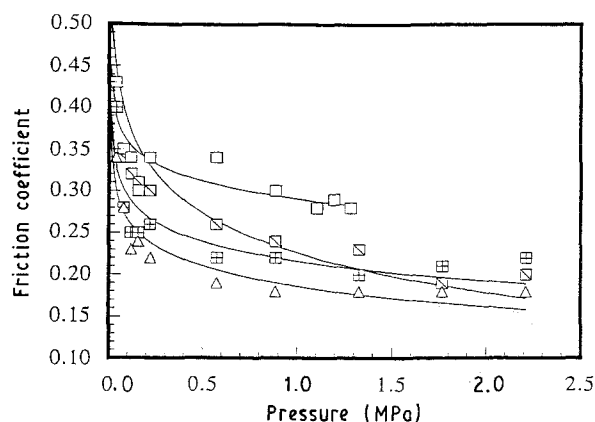


Figure 12 Friction coefficient for Kevlar Ht–metal contact as a function of pressure for (Z) steel, (H) aluminium, (Q) lead and (A) brass.

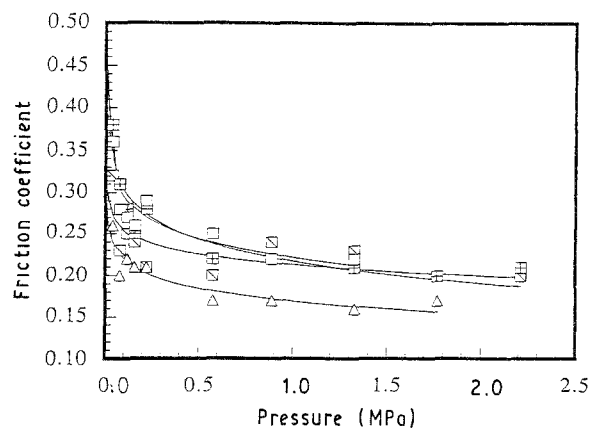


Figure 13 Friction coefficient for Kevlar 29–metal contact as a function of pressure for (Z) steel, (H) aluminium, (Q) lead and (A) brass.

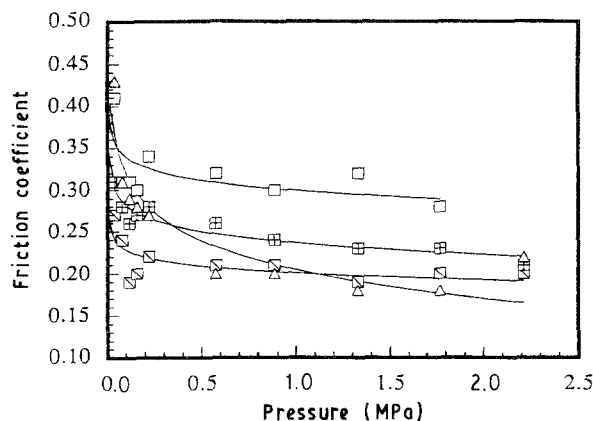


Figure 14 Friction coefficient for Kevlar 49–metal contact as a function of pressure for (Z) steel, (H) aluminium, (Q) lead and (A) brass.

figures, a general tendency of the friction coefficient to decrease with normal pressure is observed and, except for lead, for the highest pressure values tested, the value of  $\mu_d$  tends to be insensitive to pressure. In the case of lead, on the contrary, normal pressures higher than about 1.5 MPa result in large plastic deformations causing the cavities between fibres to be filled by the plastically flowing lead. Thus, an enormous increase in the friction coefficient value is expected, with respect to the values indicated in Figs 12 to 14. Finally, in Fig. 15 the friction coefficient is plotted as a

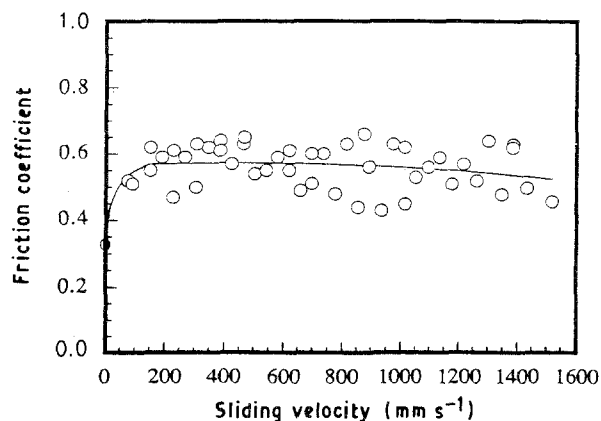


Figure 15 Friction coefficient for Kevlar Ht–steel contact as a function of sliding velocity.

function of the relative sliding velocity for the Kevlar Ht–steel interface. We see that in this case the dynamic friction coefficient is appreciably larger than the static one, and that there is little variation of the dynamic friction coefficient value with the sliding velocity.

### 3. Discussion

We can see in Fig. 3 that for Kevlar Ht and for a normal pressure value of 2.0 kPa, the friction coefficient remains nearly constant throughout the whole experiment, suggesting that a single mechanism is controlling the wear process. On the basis of the observations made, this mechanism seems to be wear abrasion, as identified in the early work by Backer [14]. For higher contact pressures, the friction coefficient increases with respect to the case of 2.0 kPa, thus suggesting that an additional wear mechanism has begun to operate. Experimental observations show that this mechanism is the plucking or shagging effect, as illustrated by Fig. 16. Such a mechanism begins to operate when fibre rupture takes place and the fibres begin to tangle, giving rise to an accelerated degradation process. As the normal pressure increases, yarns remain in closer contact, thus increasing the abrasive effects. This explains the monotonic increase in the value of the dynamic friction coefficient for a normal pressure value of 3.0 kPa, and the sudden increase of this parameter observed in Fig. 3 for a normal pressure value of 5.0 kPa. In fact, in the latter case, rupture of fibres by degradation was observed after a relatively small number of cycles. The conclusions stated above may also be drawn from Fig. 4, where a linear relationship fits the experimental data very well for a normal pressure value of 2.0 kPa, maybe corresponding to a single mechanism governing the wear process. For higher pressures the curves exhibit an upward concavity, suggesting that different wear mechanisms have now appeared.

The wear velocity curves (volume loss per unit normal load) shown in Fig. 5 for Kevlar Ht seem to fit relatively well with straight lines. However, we see that the wear velocity is about ten times greater in the cases of 3.0 and 5.0 kPa than for the case of 2.0 kPa. This

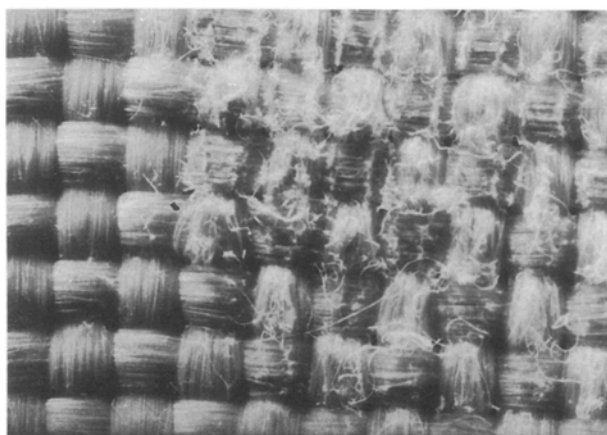


Figure 16 Kevlar Ht fabric before (left) and after (right) a dynamic wear test of fabric–fabric contact.

fact supports the conclusion that different wear mechanisms are present in both situations, as explained in the previous paragraph. It is also seen that the change of the mechanism controlling the wear process has a much more violent effect on the volume loss of material than on the friction coefficient, which increases in a more moderate manner. The specific wear curves depicted in Fig. 6 confirm the main aspects stated above.

The friction coefficient curves shown in Fig. 7 reveal some interesting points. In effect, we observe that for Kevlar Ht the dynamic friction coefficient varies little, but tends initially to decrease with the sliding distance, i.e., the dynamic friction coefficient is lower than the static one. This may be due to the generation of debris during the experiment, which acts as a lubricant. For Kevlar 49 and Kevlar 29, in contrast, the friction coefficient tends initially to increase with the sliding distance, i.e., the dynamic friction coefficient is higher than the static one. For larger sliding distance values, the dynamic friction coefficient tends to remain relatively constant. This behaviour is difficult to explain, since Figs 8, 9 and 10 reveal a very similar behaviour for the three fabrics studied here, thus suggesting that the same wear mechanism is present in the three cases. So, the increase in the dynamic friction coefficient with respect to the static value for Kevlar 29 and Kevlar 49 may be attributed to surface degradation, accompanied by a virtually null lubricant effect of the debris for these two fabrics.

The friction coefficients for aramid–metal contact shown in Figs 12 to 14 show some interesting features. The friction coefficient for aramid–lead contact, for instance, has a very similar behaviour for both Kevlar Ht and Kevlar 49, but for Kevlar 29 it decreases to appreciably lower values. This may be due to the fact that the Kevlar 29 fabrics used in this work are more closely woven, thus reducing the tendency of lead to flow plastically within the inter-yarn voids of the fabric. This aspect of lead behaviour is illustrated in Fig. 17. In Fig. 17a we can see the plastically deformed surface of the lead specimens used in the wear experiments, while Fig. 17b shows the lead core of a

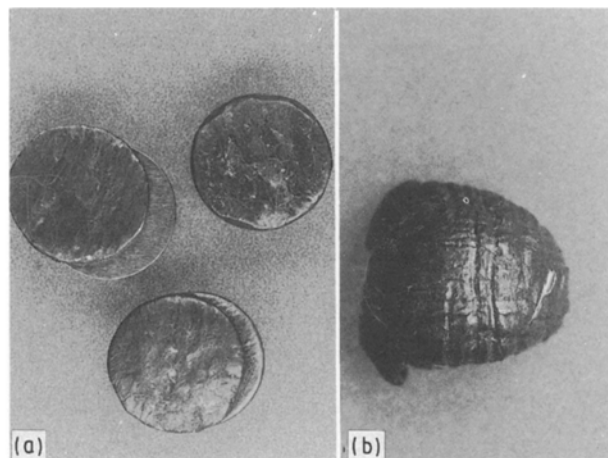


Figure 17 (a) Deformed lead specimens after dynamic wear tests; (b) deformed lead core of a Magnum .357 projectile after impact on Kevlar body armour.

Magnum .357 projectile after impact on Kevlar body armour, showing elongated indentations clearly due to lead punching by the aramid yarns. The other three materials exhibit a more or less similar behaviour for the three types of aramid fabric, the friction coefficient decreasing and tending to a roughly constant value as the normal pressure increases. This behaviour may be explained by the fact that as the pressure increases, metal comes in closer contact with the fabric, and metal asperities may generate larger amounts of fabric debris, and hence a larger lubricant effect, thus causing a decrease in the friction coefficient value. In Fig. 15 we can see that the dynamic friction coefficient is higher than the static one for the Kevlar Ht-steel interface. This behaviour may be due to enhanced surface degradation with increasing sliding velocity.

Finally, it is worth noting that in dealing with the impact of medium- and low-calibre ammunition on body armours, high impact pressures of the order of 500 MPa may be reached. In this situation, and in spite of the short duration of the impact process (about 250  $\mu$ s), important friction and wear effects take place in the fibres. Since conventional testing techniques allow an investigation of such effects at much lower pressures than those of impact problems, more effort must be directed to the development of new testing techniques at high pressures and high loading rates.

#### 4. Conclusions

This paper presents a set of results on the friction and wear behaviour of Kevlar Ht, Kevlar 49 and Kevlar 29 aramid fabrics. Both Kevlar mutual contact and metal-Kevlar contact were considered for steel, aluminium, lead and brass. The friction and wear properties have been characterized for the above interfaces in the low pressure range, a few kPa for aramid fabric mutual friction and about 1 MPa for aramid-metal friction. To obtain data which could be reliably ap-

plied to a numerical simulation of projectile impact on aramid fabric body armours, experimental techniques for determining the friction and wear behaviour at high pressures and high loading rates should be developed.

#### Acknowledgements

The authors are indebted to the Research and Development department of INDUYCO S.A. (Madrid), for the technical collaboration and the financial support of this work.

#### References

1. W.J. LYONS, "Impact Phenomena in Textiles" (MIT Press, Cambridge, Massachusetts, 1963) p. 159.
2. "Ballistics Technology of Lightweight Armor", AMMRC TR 73-47 (US Army Materials and Mechanics Research Command, Watertown, Massachusetts, 1979).
3. R.A. PROSSER, *Textile Res. J.* **3** (1988) 61.
4. C.M. LEECH and B.A. ADEYEFA, *Comp. Struct.* **15** (1982) 423.
5. D.K. ROYLANCE, *J. Appl. Mech.* **40** (1973) 143.
6. C.L. WARFIELD and B.L. SLATEN, *Textile Res. J.* **4** (1989) 201.
7. J. AMIRBAYAT and W.D. COOKE, *ibid.* **8** (1989) 469.
8. P.H. BRORENS, J. LAPPAGE, J. BEDFORD and S.L. RANFORD, *ibid.* **2** (1990) 126.
9. N. SUNG and N.P. SUH, *Wear* **53** (1979) 129.
10. R. RAMESH, R. KISHORE and R. RAO, *ibid.* **89** (1983) 131.
11. B. VISHWANATAH, A.P. VERMA and C.V. RAO, *Composites* **21** (1990) 331.
12. C. ZWEBEN and J.C. NORMAN, *SAMPE Quart.* **10** (1976) 1.
13. B.J. BRISCOE and F. MOTAMEDI, *Textile Res. J.* **12** (1990) 697.
14. S. BACKER, *ibid.* **21** (1951) 453.

Received 18 November 1991  
and accepted 14 August 1992